Supplementary Information for the article:

Heinrich event 1: an example of dynamical ice-sheet reaction to oceanic changes

Jorge Álvarez-Solas[1,2]**, Marisa Montoya**[1,3]**, Catherine Ritz**[4]**, Gilles Ramstein**[2]**,
Sylvie Charbit**[2]**, Christophe Dumas**[2]**, Kerim Nisancioglu**[5]**, Trond Dokken**[5]**, and
Andrey Ganopolski**[6]

[1]Dpto. Astrofísica y Ciencias de la Atmósfera, Universidad Complutense, Madrid, Spain
[2]LSCE/IPSL, CEA-CNRS-UVSQ, UMR 1572, CEA Saclay, Gif-sur-Yvette, France
[3]Instituto de Geociencias (UCM-CSIC), Facultad de Ciencias Físicas, Madrid, Spain
[4]Laboratoire de Glaciologie et de Géophysique de l'Environnement, CNRS, Saint Martin
d'Hères, France
[5]Bjerknes Centre for Climate Research, Bergen, Norway
[6]Potsdam Institute for Climate Impact Research, Potsdam, Germany

Correspondence to: J. Alvarez-Solas
(jorge.alvarez.solas@fis.ucm.es)

1 Numerical reconstruction of the Northern Hemisphere ice sheets

1.1 The indexation method

In order to obtain the LGM ice-sheet distribution, the GRISLI three-dimensional ice-sheet model of the Northern Hemisphere Ritz et al. (2001); Peyaud et al. (2007) was forced from 130 kyr BP to present using a time-varying climatology (for summer and mean annual surface air temperature as well as mean annual precipitation) for the last glacial cycle. The latter was reconstructed using snapshots from the former CLIMBER-3α LGM climate simulation as well as from a preindustrial climate simulation Montoya and Levermann (2008), and an interpolation through time between these snapshots using a glacial index calibrated against the GRIP $\delta^{18}O$ record. To minimize errors due to model deficiencies, a perturbative method is used. The time-varying surface air temperature is thus given by:

$$T(t) = T_{CLIM} + (1 - \alpha(t)) \times (T_{LGM} - T_{CTRL}), \tag{1}$$

while precipitation results from:

$$P(t) = P_{CLIM} \times (1 - \alpha(t)) \times (P_{LGM}/P_{CTRL}), \tag{2}$$

where f_{CLIM} represents the present-day climatology, f_{LGM} and f_{CTRL} are the LGM and control snapshots, respectively, and $\alpha(t)$ is the glacial index. For the present $\alpha = 1$ and the present-day climatology is recovered. The same applies to 130 kyr BP. For the LGM $\alpha = 0$ and we recover the present-day climatology corrected by the simulated anomalies. Additional corrective factors accounting for the surface elevation difference between past and present are also considered. Temperature fields are thus corrected by using a lapse rate index, while the impact of the temperature difference between past and present on the precipitation is accounted for by an exponential term. The procedure is detailed in Charbit et al. (2007) and is based on the assumption that the spatial patterns of temperature and precipitation variations over the last glacial period linearly change with time and, therefore, climatic variations follow the GRIP $\delta^{18}O$ record. This approach cannot capture the likely effects of an evolving ice sheet geometry on atmospheric and oceanic circulations. However, this method has been revealed to be very

helpful to reconstruct the past Northern ice sheets, especially around the LGM period Marshall et al. (2000, 2002); Charbit et al. (2002, 2007).

1.2 Implementation of the basal dragging dependence on sediments

An important improvement present in GRISLI with respect to models which are only based on the Shallow Ice Approximation (SIA) is the fact that areas where the basal ice is at the melting point, whereby ice flow occurs in presence of water, are treated in the model under the shallow ice shelf/stream approximation proposed by MacAyeal (1989), which allows for a more proper representation of ice streams than under the pure SIA. In this way, the ice streams velocities depend on the basal dragging coefficients τ, that are function of the bedrock characteristics and effective pressure:

$$\vec{\tau_b} = -\nu^2 N \vec{U_b} \tag{3}$$

where N represents the effective pressure (balance between ice and water pressure) and ν^2 an empirical parameter with a typical value of $0.9 \ 10^{-5}$ has been adjusted in order to fit the Antarctic simulated ice velocities to those given by satellite observation. However, this cannot be done for Northern Hemisphere glacial simulations. We decide to account for this uncertainty by considering a set of four different values of the ν^2 parameter:

$$\nu^2 = 1, 2, 10 \times 10^{-4} \ (dimensionless) \tag{4}$$

where ν^2 represents the basal friction coefficient in ice streams.

Ice streams are therefore treated in GRISLI as ice shelves with basal dragging. The challenge consists on appropiately calculate the basal friction in each point. Areas in presence of soft sediments will allow less friction than areas in where the basal ice is directly in contact with the bedrock. Here we accounted on this effect by allowing the presence of a potential ice stream only in regions with an enough thickness of sediments Mooney et al. (1998).

1.3 The basal melting computation

It has been largely suggested that the processes allowing ice surges of the ice sheets and dramatic calving episodes are closely related with the oceanic behaviour Hulbe et al. (2004); Shaffer et al. (2004); Flückiger et al. (2008). The floating part of the ice sheets (ice shelves) constitutes the component where this link has more relevance. The mass balance of the ice shelves is determined by the ice flow upstream, surface melt water production, basal melting and calving. Basal melting under the ice shelves represents the biggest unknown parameter in paleoclimate simulations involving ice sheets and ice shelves. Beckman and Goose Beckmann and Goosse (2003) suggested a law to compute this basal melting rate based on the heat flux between the ocean and floating ice. This method is particularly helpful for regional ocean/ice shelves models. Following their equations, under present-day climate conditions, the net basal melting rate can be well constrained in high resolution coupled ocean-shelf models:

$$B = \frac{\rho_o c_{po} \gamma_T}{\rho_i L_i} (T_o - T_f) A_{eff}, \tag{5}$$

where T_o is the (subsurface-) ocean temperature, T_f is the freezing point temperature at the base of the ice-shelf Beckmann and Goosse (2003) and A_{eff} is an effective area for melting. Basal melting resulting from this equation would be appropriate for a high resolution ocean/ice shelf. However, this method remains controversial Olbers and Hellmer (2010) and due to the coarse ocean model resolution, the processes involved are not well resolved. Therefore, due to the time and spatial scales involved in our experiments, the latter expression can thus be rewritten as follows:

$$B = \kappa (T_o - T_f). \tag{6}$$

To take the associated uncertainty into account we simply explore the response of our model to a large values range of this parameter:

$$\kappa = 0.2, 0.5, 1 \, myr^{-1} K^{-1}. \tag{7}$$

Note here for simplicity variations of the annual mean subsurface ocean temperature T_o throughout the last glacial cycle were neglected. Thus, the mean annual subsurface ocean temperature

4

T_o corresponding to the LGM snapshots was used instead of an interpolated value based on the GRIP δ^{18}O as is done for the atmospheric fields. This parameter determines the magnitude of basal melting changes as a function of oceanic temperatures. The basal melting amplitude will determine not only the presence and thickness of ice shelves, but also the capability of ice sheets to advance over the coast (i.e. grounded line migration). Thus, starting from the last interglacial period (130 kyr BP), different values of κ determine different configurations of the spatial distribution of the Northern Hemisphere ice sheets at the LGM.

2   Sensitivity experiments

Together with the abovementioned range of values considered for κ, this yields a set of $n = 9(3 \times 3)$ simulations, corresponding to all possible combinations of values of the former parameters, each of which yields a different configuration of the Northern Hemisphere ice sheets at 21 kBP This method allows us to explore the sensitivity of the initial ice-sheet configuration to the former parameters and to assess the interaction between ice sheets and ocean circulation over a wide phase space of the system initial conditions.

The Northern Hemisphere grounded ice volume increases monotonically with increasing drag parameter ν^2, reflecting the fact that the ice-streams are less active but is insensitive to the basal melting parameter κ A similar result applies to the Laurentide grounded ice-volume By contrast, the corresponding floating ice volumes decrease by roughly one order of magnitude with increasing κ. Its dependence on ν^2 for a given κ is not monotonical due to the fact that there are two competing processes: Low dragging coefficients (high velocities) favor the occurrence of a fast and relatively shallow ice shelf, while strong friction coefficients implies slower ice streams and thicher ice shelves.

For the lowest range of basal melting parameter κ, a huge ice shelf is simulated in the Labrador Sea. Note that the spatial distribution of ice streams is in very good agreement with other studies based on reconstruction methods Winsborrow et al. (2004). On the other hand, the very active ice streams flowing from the Hudson Bay/Strait region favor the occurrence of a few partially embayed ice shelves which spatial shape shows a good concordance with that

expected by Hulbe Hulbe et al. (2004). This simulation that has been considered as the standard one in the main text, corresponds to $\kappa = 0.5$, $\nu^2 = 10^{-4}$. In all cases the results obtained should be considered as underestimating the total ice-volume, because the strong AMOC state, with a warmer North Atlantic, was used to scale the GRIP data and/or because in the GRISLI version used herein the presence of sediments is an additional criterium to determine whether a certain area should behave as an ice-stream or not. Under this new criterium, areas potentially treated as ice streams increase resulting in a more reactive ice sheet especially in Laurentide where the maximum thickness is always below the ICE-5G reconstruction.

3   On the effects of ocean circulation changes on LIS dynamics

We herein show that modest freshwater fluxes originated in melting of the Fennoscandian ice-sheet around 19 kyr BP might have induced a reduction of the Atlantic meridional overturning circulation (AMOC) resulting in subsurface warming in the northern north Atlantic and the Labrador sea which leads to melting of the Hudson Strait ice shelf and thereby to a Heinrich (H) event. We hypothesize such a mechanism operated during H1.

Recently, deep sea sediment core data from the Nordic Seas have suggested enhanced calving from the Fennoscandian ice-sheet at ca. 19 kBP leading to enhanced freshwater flux into the Nordic Seas. In order to analyze the possible climatic impacts of such enhanced freshwater flux, an idealized step-function surface freshwater flux perturbation with amplitude varying between A = 0.01-0.5 Sv during a period Δt = 10-100 years was imposed in the northern North Atlantic from 61-63°N and 6°W-5°. This implies, at most, a sea-level rise of up to ca. 1.8 m in as much as 100 years. The latter is consistent with sea-level reconstructions, which show no evidence of a substantial meltwater input at the time (from 15-21 kyr BP) Hanebuth et al. (2000); Peltier and Fairbanks (2006).

Following the freshwater flux perturbation, the surface salinity decreases in the Nordic Seas (not shown), reducing convection in this region. The negative surface salinity anomalies are propagated into the Labrador Sea by the North Atlantic subpolar gyre, thereby contributing to reduce convection as well as deep water formation in the latter region as well.

6

The responses all basically cluster around two modes: for relatively weak forcing ($\Delta t \leq 20$ year) the AMOC strength is reduced from ca. 22 Sv to ca. 16 Sv and recovers several centuries after the surface freshwater forcing end. For stronger forcing ($\Delta t > 20$ yr), the AMOC is reduced to a value close to that of the stadial state (12 Sv) and does not recover after the freshwater forcing suppression within 2000 years. Each of these two modes shows a different pattern of North Atlantic convection after several centuries, with the less perturbed mode showing a more modest reduction.

The weakened AMOC translates into a reduction of northward heat transport to high northern latitudes and thereby mean annual SSTs and SATs in the northern North Atlantic and Greenland decrease by up to 4 K.

The 9 Northern Hemisphere ice sheet configurations at 18 kyr BP have been equally perturbed by the oceanic subsurface warming resulting from the shift between a strong and a weak AMOC state (Figure 1).

Our results extend those of prevoius works in two ways. First, we have shown that a modest perturbation originated in the Fennoscandian ice-sheet, which cannot readily be identified in the sea-level reconstructions, can lead to decrease of deep water formation in the north Atlantic resulting in subsurface warming of several degrees. Second, using a state-of-the art ice-sheet model of the Northern Hemisphere including a parameterization of ice shelves we have shown that, within a wide parameter range, the latter subsurface warming can lead to a collapse of the ice-shelf in Hudson Strait and inland ice-streams acceleration possibily explaining H1.

References

Beckmann, A. and Goosse, H.: A parameterization of ice shelf-ocean interaction for climate models, Ocean Modelling, 5, 157–170, 2003.

Charbit, S., Ritz, C., and Ramstein, G.: Simulations of Northern Hemisphere ice-sheet retreat: sensitivity to physical mechanisms involved during the Last Deglaciation, Quaternary science reviews, 21, 243–265, 2002.

Charbit, S., Ritz, C., Philippon, G., Peyaud, V., and Kageyama, M.: Numerical reconstructions of the

Northern Hemisphere ice sheets through the last glacial-interglacial cycle, Clim, Clim. Past, 3, 15–37, 2007.

Flückiger, J., Knutti, R., White, J., and Renssen, H.: Modeled seasonality of glacial abrupt climate events, Clim. Dyn., doi:10.1007/s00382-008-0373-y, 2008.

Hanebuth, T., Stattegger, K., and Grootes, P.: Rapid flooding of the Sunda Shelf: a late-glacial sea-level record, Science, 288, 1033, 2000.

Hulbe, C., MacAyeal, D., Denton, G., Kleman, J., and Lowell, T.: Catastrophic ice shelf breakup as the source of Heinrich event icebergs, Paleoceanography, 19, 2004.

MacAyeal, D.: Large-scale ice flow over a viscous basal sediment- Theory and application to ice stream B, Antarctica, Journal of Geophysical Research, 94, 4071–4087, 1989.

Marshall, S., Tarasov, L., Clarke, G., and Peltier, W.: Glaciological reconstruction of the Laurentide Ice Sheet: physical processes and modelling challenges, Canadian Journal of Earth Sciences, 37, 769–793, 2000.

Marshall, S., James, T., and Clarke, G.: North American ice sheet reconstructions at the Last Glacial Maximum, Quaternary Science Reviews, 21, 175–192, 2002.

Montoya, M. and Levermann, A.: Surface wind-stress threshold for glacial Atlantic overturning, Geophys. Res. Lett., 35, L03 608, doi:10.1029/2007GL032 560, 2008.

Mooney, W., Laske, G., and Masters, T.: CRUST 5.1: A global crustal model at 5×5, Journal of Geophysical Research-Solid Earth, 103, 1998.

Olbers, D. and Hellmer, H.: A box model of circulation and melting in ice shelf caverns, Ocean Dynamics, 60, 141–153, 2010.

Peltier, W. and Fairbanks, R.: Global glacial ice volume and Last Glacial Maximum duration from an extended Barbados sea level record, Quaternary Science Reviews, 25, 3322–3337, 2006.

Peyaud, V., Ritz, C., and Krinner, G.: Modelling the Early Weichselian Eurasian Ice Sheets: role of ice shelves and influence of ice-dammed lakes, Clim, Past, 3, 375–386, 2007.

Ritz, C., Rommelaere, V., and Dumas, C.: Modeling the evolution of Antarctic ice sheet over the last 420,000 years: Implications for altitude changes in the Vostok region, Journal of Geophysical Research-Atmospheres, 106, 31 943–31 964, 2001.

Shaffer, G., Olsen, S., and Bjerrum, C.: Ocean subsurface warming as a mechanism for coupling Dansgaard-Oeschger climate cycles and ice-rafting events, Geophys. Res. Lett, 31, 2004.

Winsborrow, M., Clark, C., and Stokes, C.: Ice streams of the Laurentide ice sheet, Géographie Physique et Quaternaire, 58, 269, 2004.
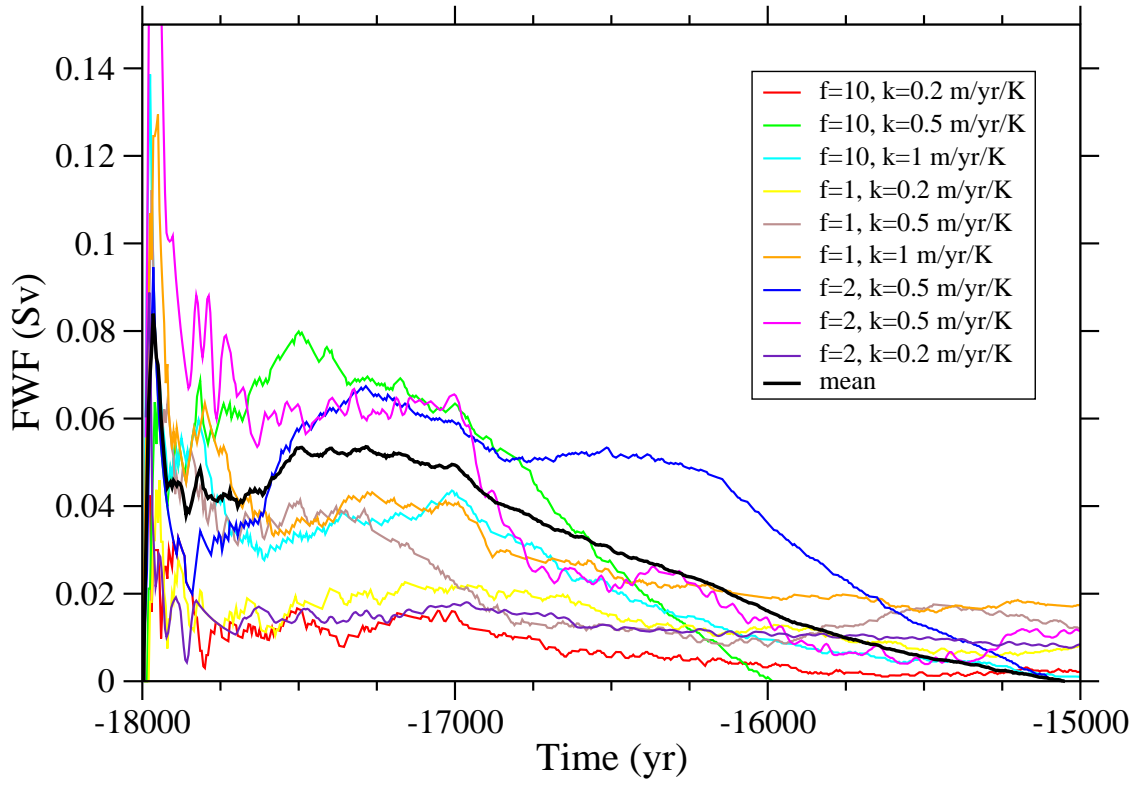
Fig. 1. Iceberg calving (in Sv) derived from the effects of the oceanic subsurface warming on the dynamic behavior of the Laurentide ice sheet for nine different configurations of the model.